

# Analytical Methods

Accepted Manuscript



This is an *Accepted Manuscript*, which has been through the Royal Society of Chemistry peer review process and has been accepted for publication.

*Accepted Manuscripts* are published online shortly after acceptance, before technical editing, formatting and proof reading. Using this free service, authors can make their results available to the community, in citable form, before we publish the edited article. We will replace this *Accepted Manuscript* with the edited and formatted *Advance Article* as soon as it is available.

You can find more information about *Accepted Manuscripts* in the [Information for Authors](#).

Please note that technical editing may introduce minor changes to the text and/or graphics, which may alter content. The journal's standard [Terms & Conditions](#) and the [Ethical guidelines](#) still apply. In no event shall the Royal Society of Chemistry be held responsible for any errors or omissions in this *Accepted Manuscript* or any consequences arising from the use of any information it contains.

Cite this: DOI: 10.1039/c0xx00000x  
www.rsc.org/xxxxxx

ARTICLE TYPE

Colorimetric detection of mercury ion using MnO<sub>2</sub>nanorods as enzyme mimics

Haiguang Yang, YuhaoXiong, Peng Zhang, Lingjing Su, Fanggui Ye\*

Received (in XXX, XXX) Xth XXXXXXXXXX 20XX, Accepted Xth XXXXXXXXXX 20XX  
DOI: 10.1039/b000000x

In this study, a simple and novel “off-on” colorimetric sensor for the detection of mercury ion (Hg<sup>2+</sup>) in aqueous solution was developed. The homogeneous MnO<sub>2</sub> nanorods as oxidase-like mimetics could catalyze the oxidation of 3, 3', 5, 5'-tetramethylbenzidine (TMB) into a blue colored cation radical without the requirement for additional oxidizing agents. Glutathione (GSH) could successfully hinder the cation radical producing and restore them to colourless TMB molecules. Hg<sup>2+</sup> had a strong affinity to thiolated compounds. If GSH and Hg<sup>2+</sup> were pre-incubated, the solution would be recovered to blue colored solution in the presence of MnO<sub>2</sub> nanorods. Based on this phenomenon, a simple and rapid colorimetric path for the sensing of Hg<sup>2+</sup> was developed. A good linear relationship could be obtained from 0.1 to 8.0 μM. The limit of detection was estimated to be 0.08 μM. The proposed method was successfully applied for the determination of Hg<sup>2+</sup> in real water samples with recoveries ranging from 82% to 114%. And this method was allowed for the monitoring of Hg<sup>2+</sup> directly with naked eyes.

1. Introduction

The monitoring of toxic metal ions in aquatic ecosystems is an important issue owing to its adverse effect on human health and the environment.<sup>1</sup> Mercury (II) ion (Hg<sup>2+</sup>) is recognized as one of the most toxic metal ions in the world, and it mainly release to the atmosphere from power plants, burning fossil fuels, and solid waste incineration.<sup>2</sup> This pollutant is a recognized hazardous contaminant that accumulates in living organisms. Exposure to low levels of Hg<sup>2+</sup>, mostly from natural waters, humans can be severely harmed and suffered from brain, heart, kidney, lung, and immune system.<sup>3</sup> Therefore, it is necessary to develop a facile and rapid method for monitoring of trace levels of Hg<sup>2+</sup> in environmental samples with good sensitivity. There are various classical methods have been developed for the determination of Hg<sup>2+</sup>, including cold vapor atomic absorption spectroscopy,<sup>4</sup> cold vapor generation inductively coupled plasma mass spectrometry,<sup>5</sup> chemiluminescence,<sup>6</sup> electrochemical,<sup>7</sup> chromatographic<sup>8</sup> and fluorometric methods.<sup>9</sup> These methods exhibited sensitive and very specific, but required complicated, time-consuming sample preparation and treatments, and expensive, sophisticated instruments that limit their further applications. Colorimetric detection would be a more desirable method due to its low cost, simple and rapid detection procedures. Because the changes of colour can be seen by the naked eyes, colorimetric sensing does not require expensive or complicated instrumentation and can be applied to field analysis.<sup>10</sup> In particularly, enzyme-like nanomaterials-based sensors have already emerged as an important colorimetric tool due to their high catalytic properties, stability, low cost, relatively simple preparation and storage.<sup>11</sup> Therefore, they with a wide range of practical applications are becoming a significant field for

different intentions.<sup>12</sup> Recently, several studies have been reported for the colorimetric detection of Hg<sup>2+</sup> in aqueous solution by exploiting the peroxidase mimetic property.<sup>13-16</sup> For instance, Huang et al.<sup>13</sup> developed a sensitive label-free colorimetric method for Hg<sup>2+</sup> based on mercury-stimulated peroxidase mimetic activity of gold nanoparticles. Wang et al.<sup>14</sup> proposed a high-throughput colorimetric assay for Hg<sup>2+</sup> in blood and wastewater based on the mercury-stimulated catalytic activity of small silver nanoparticles in a temperature-switchable gelatin matrix. Mohammadpour et al.<sup>15</sup> reported a label free on-off colorimetric sensor for Hg<sup>2+</sup> determination based on carbon nanodots as enzyme mimics. Fu et al.<sup>16</sup> designed a BSA-stabilized Pt nanozyme for colorimetric detection of Hg<sup>2+</sup> ions in aqueous solution. Although these methods are sensitive and selective for Hg<sup>2+</sup> determination, they usually require an additional destructive and unstable H<sub>2</sub>O<sub>2</sub> as oxidant. In contrast, oxidase mimetics could oxidize substrates using oxygen as a green oxidant without the need of H<sub>2</sub>O<sub>2</sub>. Wu et al.<sup>17</sup> used Au@Pt nanorod oxidase mimics for visual detection of Hg<sup>2+</sup> without the need of H<sub>2</sub>O<sub>2</sub>. Wang et al.<sup>18</sup> developed a simple and fast colorimetric detection of Hg<sup>2+</sup> based on the oxidase-like activity of citrate-capped silver nanoparticles. Recently, manganese dioxide (MnO<sub>2</sub>) has attracted considerable attention due to low cost, high activity/stability, nontoxicity and abundant availability.<sup>19-21</sup> In 2012, Zhang et al.<sup>22</sup> found that MnO<sub>2</sub> nanomaterials possessed an oxidase-like activity. Afterward, Lv et al.<sup>23</sup> reported that BSA-MnO<sub>2</sub> nanoparticles exhibited high oxidase-like activities. What's more, they used BSA-MnO<sub>2</sub> nanoparticles as oxidase-like mimetics for colorimetric detection of glutathione (GSH) in human blood serum based on the reduction of oxidized TMB.<sup>24</sup> More recently, we prepared

Analytical Methods Accepted Manuscript

magnetic core-shell nanoflower  $\text{Fe}_3\text{O}_4@\text{MnO}_2$  as reusable oxidase mimetics for colorimetric detection of phenol.<sup>25</sup> These findings would be open up a new field for  $\text{MnO}_2$  applications. To the best of our knowledge, no studies on exploration of oxidase-like activity of  $\text{MnO}_2$  for colorimetric detection of  $\text{Hg}^{2+}$  have been reported so far.

Herein, we developed novel  $\text{MnO}_2$  nanorods as oxidase-like mimetic by reducing  $\text{MnO}_4^-$  with reductants. We used homogeneous  $\text{MnO}_2$  nanorods to catalyze the oxidation reaction of TMB without the requirement for additional oxidizing agents. Once TMB was oxidation, a blue colored cation radical was generated. GSH could successfully cause a decrease cation radical generation by means of its strong radical restoration ability. Inspired by this, we designed a simple and rapid “off-on” colorimetric sensor for  $\text{Hg}^{2+}$  in aqueous solution based on the strong affinity between thiolated compounds and  $\text{Hg}^{2+}$ . The turn on sensing mode in here maybe reduce back ground signals and improve the system sensitivity.

## 2. Experimental

### 2.1. Materials

All chemicals are obtained from commercial source and used without further purification. Unless otherwise stated, all chemicals are of analytical reagent grade. Sodium acetate (NaAc), acetic acid (HAc) and potassium permanganate ( $\text{KMnO}_4$ ) were purchased from Shantou Xilong Chemical Factory (Guangdong, China). TMB and GSH were obtained from Sigma-Aldrich (USA). Ultrapure water (18.2  $\text{M}\Omega\text{ cm}$ ) was produced by a Millipore purification system (Bedford, MA, USA) and used to prepare all aqueous solutions.

### 2.2. Apparatus

Absorption spectra were recorded on a model Cary 60 spectrophotometer (Agilent, USA). Scanning electron microscopy (SEM) was carried out using a FEI Quanta 200 FEG SEM (Philips, Netherlands). X-ray diffraction (XRD) patterns of the samples were recorded on a X'Pert PRO diffractometer (PANalytical, The Netherlands) with  $\text{Cu K}\alpha$  radiation ( $\lambda=0.15418\text{ nm}$ ).

### 2.3. Preparation of $\text{MnO}_2$ nanorods

The  $\text{MnO}_2$  nanorods were synthesized by a chemical reduction method. 50 mg  $\text{KMnO}_4$  was added to a 25 mL beaker containing 5 mL ultrapure water. Then, 50  $\mu\text{L}$  30%  $\text{H}_2\text{O}_2$  and 50  $\mu\text{L}$  40% hydrazine hydrate were added and the solution was stirred vigorously for 5 min by the magnetic stirrer. A brown colloid was observed. After the obtained emulsion standing for a moment, the supernatant was removed, and washed for five times with ultrapure water to remove the unreacted reagent.

### 2.4. Detection of mercury ion

The detection of  $\text{Hg}^{2+}$  was performed according to the following steps: at room temperature, 100  $\mu\text{L}$  400  $\mu\text{M}$  GSH and different concentrations of  $\text{Hg}^{2+}$  solutions were added in 1 mL of 0.2 M NaAc-HAc buffer solution (pH 4.5). After 5 min of incubation, 120  $\mu\text{L}$  1.0 mM TMB and 120  $\mu\text{L}$  0.19 mg/mL  $\text{MnO}_2$  were added. The mixtures were finally diluted to 2 mL using ultrapure water and incubated for another 10 min at 25°C. Finally, a model Cary

60 spectrophotometer was applied to determine the absorption spectra of the solutions.

### 2.5. Analysis of real samples

Pool water and Li River water samples were analyzed as the real samples without any filtration and treatments. 20 mL the pool water and 20 mL Li River water samples were respectively diluted by acetate buffer (pH =4.5, 0.4 M) to 40 mL. 2.5 mL of these solutions were added to 5 mL the centrifugal tube, 100  $\mu\text{L}$  of 600  $\mu\text{M}$  GSH and different concentrations of  $\text{Hg}^{2+}$  solutions were spiked. After 5 min of incubation, 120  $\mu\text{L}$  of 1.5 mM TMB and 180  $\mu\text{L}$  of 0.19 mg/mL  $\text{MnO}_2$  were added. The final volume was 3 mL and incubated for another 10 min at 25°C. The mixed solutions were analyzed with the proposed method and obtained the percent recovery values.

## 3. Results and discussions

### 3.1. Investigation the oxidase-like activity of $\text{MnO}_2$ nanorods

In order to improve the dispersity of as-prepared  $\text{MnO}_2$  nanorods in aqueous solution, the nanorods were sonicated for 10 min. The results showed that  $\text{MnO}_2$  nanorods had good water dispersibility after sonication (Fig.1a, b). The as-synthesized samples were studied by scanning electron microscopy (SEM) images (Fig.1c,

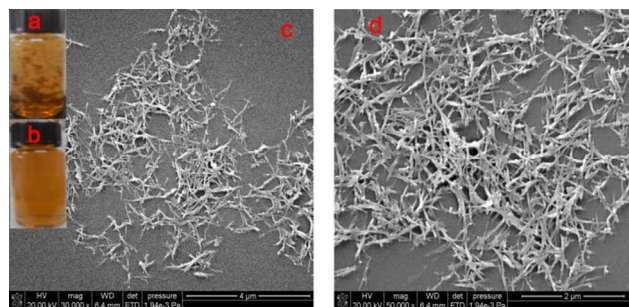


**Fig. 1** The dispersion of as-prepared  $\text{MnO}_2$  nanorods without sonication (a) and with (b) standing for 35 min after sonication. The SEM images of the as-prepared  $\text{MnO}_2$  nanorods (c, d).

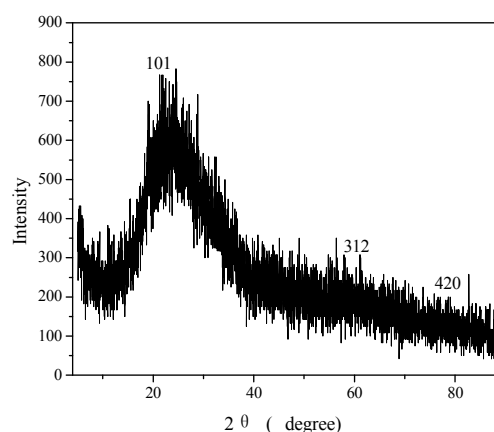


**Fig. 2** The XRD patterns of as-prepared  $\text{MnO}_2$  nanorods

d), which present rod-like morphology for  $\text{MnO}_2$ . The diameter was about 15-25 nm and the length was about 100-200 nm of these nanorods. The small size could benefit for the  $\text{MnO}_2$  nanorods dispersed in water and with high catalytic performance of  $\text{MnO}_2$  nanorods as an oxidase mimic. The  $\text{MnO}_2$  nanorods stored in water at room temperature also showed a very good stability. The phase and crystallographic structure of as-prepared  $\text{MnO}_2$  nanorods were determined by powder XRD. As shown in Fig. 2, the diffraction peaks can be well indexed with  $\text{MnO}_2$  (JCPDS card no. 39-0375).

The oxidase-like catalytic activity of  $\text{MnO}_2$  nanorods were investigated by colorimetric tests with the TMB substrate. When TMB or  $\text{MnO}_2$  nanorods were added in acetate buffer, we can observe that there were not absorption peaks at 370 nm and 652 nm. However, upon putting  $\text{MnO}_2$  nanorods, the TMB solution changed from colorless to a typical blue color and appeared two absorption peaks at 370 nm and 652 nm. These results indicated that  $\text{MnO}_2$  nanorods exhibited an intrinsic oxidase-like catalysis ability to transform TMB to a blue colored product in the absence of  $\text{H}_2\text{O}_2$  (Fig. 3).

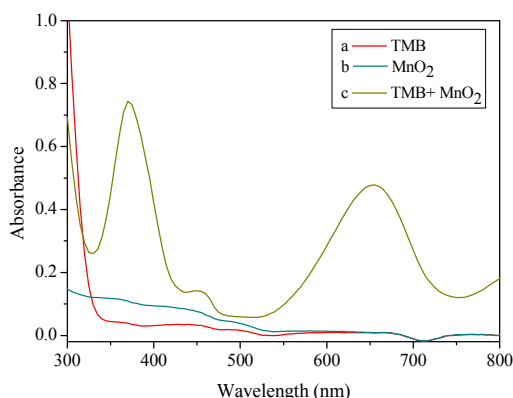


**Fig. 3** The absorption spectra of the acetate buffer in the presence of TMB (a),  $\text{MnO}_2$  (b), TMB and  $\text{MnO}_2$  (c).

### 3.2. Colorimetric mechanism of the $\text{Hg}^{2+}$ determination

At room temperature, the generation of the blue colored TMB cation radical was monitored spectrophotometrically at 652 nm for the cases of  $\text{MnO}_2$  nanorods,  $\text{MnO}_2$  nanorods/GSH and  $\text{MnO}_2$  nanorods/GSH/ $\text{Hg}^{2+}$  systems. The color of the three kinds of reaction solution and the ultraviolet visible absorption spectroscopy were shown in Fig. 4. These results revealed that when GSH was added in the deep blue color solution, the solution faded quickly with the absorption intensity decreasing. Interestingly, if we added GSH and  $\text{Hg}^{2+}$  pre-incubated for 5 min, the light blue solution would turn back to blue solution and the absorption spectroscopy also recovered. In the reaction system, no oxidants were employed, so we supposed that the dissolved  $\text{O}_2$  might be the oxidant. In order to study whether the dissolved  $\text{O}_2$  played a role in the catalytic oxidation, we conducted two sets of experiments. The first one was made in the presence of  $\text{O}_2$ . The other was bubbling with high purity nitrogen ( $\text{N}_2$ ). The absorption spectra and the corresponding photograph were

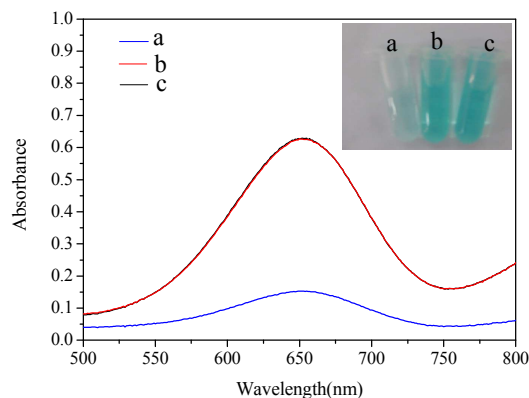


**Fig. 4** The absorption spectra of the acetate buffer in the presence of TMB,  $\text{MnO}_2$  and GSH (a), TMB,  $\text{MnO}_2$ , GSH and  $\text{Hg}^{2+}$  (b), TMB and  $\text{MnO}_2$  (c). Inset is the corresponding of the three samples color.

shown in Fig. 5. It was found that they exhibited different colour. At 652 nm, the first one's absorbance was 0.555; the other was 0.354. The obtained results indicated that the  $\text{O}_2$  in the solution effected the reaction, which is similar to some nanoparticles-based oxidase mimics reported.<sup>23, 26</sup> However, the background is quite high when  $\text{O}_2$  was displaced by  $\text{N}_2$ , indicating that  $\text{MnO}_2$  nanorods still showed catalytic ability. This catalytic activity after bubbling with high purity  $\text{N}_2$  could be attributed to chemisorbed  $\text{O}_2$ , which probably existed on the surface of  $\text{MnO}_2$  nanorods due to larger surface energy of nanomaterials.<sup>27</sup> Thus, the reaction of the oxidase-like activity of  $\text{MnO}_2$  nanorods can be described by the equation in Fig. 6b (1). We designed an "off-on" strategy in this work to detect the  $\text{Hg}^{2+}$ . It was depicted in Fig. 6. The sensor is in the "off" state in the presence of GSH, which could restore the blue TMB cation radicals to original colorless TMB molecules by its thiol functionality. This result was similar to some reported reactions,<sup>15,24,27</sup> the reaction equation was shown

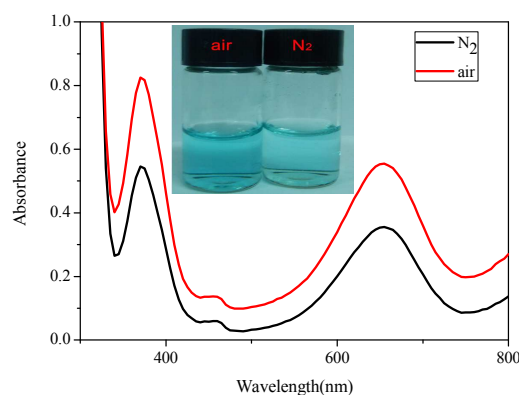


**Fig. 5** The absorption spectra of the reaction in the presence of air (red line),  $\text{N}_2$  (black line). Inset is the corresponding of the two samples' photograph.



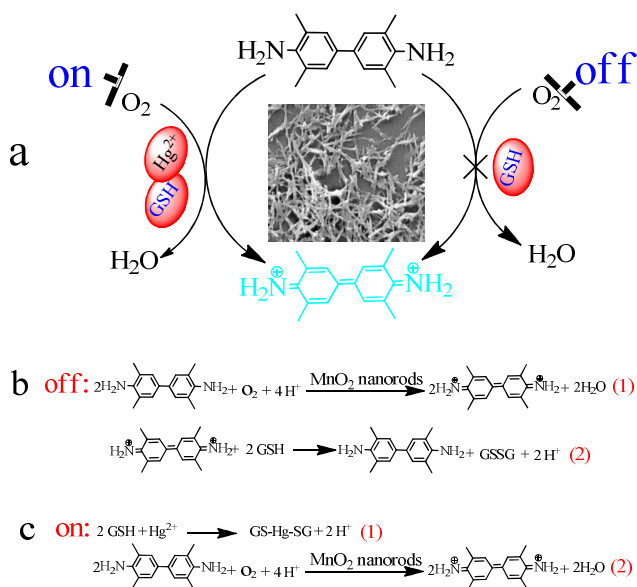


**Fig. 6** An off-on process for  $\text{Hg}^{2+}$  detection use colorimetric method.

in Fig. 6b. However, the sensor is in the “on” state in the absence of GSH due to the catalytic of oxidation process of TMB by  $\text{MnO}_2$  nanorods. Upon adding  $\text{Hg}^{2+}$  in the system of GSH/ $\text{MnO}_2$  nanorods/TMB, the deep blue solution was emerged. And the colorimetric signal was recovered obviously due to the strong affinity between  $\text{Hg}^{2+}$  and GSH. This phenomenon was believed to be due to the  $\text{Hg}^{2+}$ -thiol complexes, which had high stability constants<sup>28, 29</sup>, and the reaction equation was shown in Fig. 6c.

### 3.3. Optimization of experimental conditions.

Additional assay parameters were evaluated to further optimize the experimental protocol.  $\text{MnO}_2$  nanorods are similar to other nanomaterials-based oxidase and peroxidase mimetics, the catalytic activity of  $\text{MnO}_2$  nanorods is also dependent on pH of reaction buffer and the incubation temperature. In order to obtain the optimization of the catalytic activity of the as-prepared  $\text{MnO}_2$  nanorods, the incubation time and the concentrations of TMB were also investigated in this study as influencing factors. Mixed GSH and  $\text{Hg}^{2+}$  were pre-incubated for 5 min to ensure a

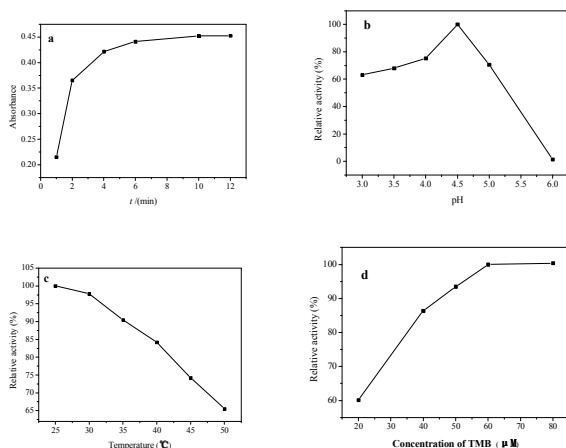


**Fig. 7** The affection of incubation time (a), the solution of the pH values (b), temperature (c), concentration of the TMB (d).

completed reaction. Then these conditions were investigated. The results were illustrated in Fig. 7a. The relative activity increased with the increase of incubation time up to 10 min, where the maximum relative activity was reached. Further increasing of incubation time did not result in an increase in absorbance. Therefore, the incubation time was chosen at 10 min for a maximum relative activity. As we all know that the pH is an important study condition in catalytic reaction, so the effect of the pH values was investigated. As shown in Fig. 7b, the relative activity first increased and then decreased with increasing pH value. The maximum relative activity was obtained when the pH value was 4.5. Therefore, the reaction solution was buffered at 4.5 for a maximum enhanced relative activity signal. The effect of reaction temperature on relative activity was shown in Fig. 7c. It can be seen that relative activity decreases with increasing temperature from 25°C to 50°C. Hence, room temperature (25°C) was taken as the suitable temperature. It can be seen from Fig. 7d that the relative activity increased with increasing the concentration of TMB. When the concentration of TMB was over 60 μM, the relative activity was constant. The results showed that the suitable concentration of TMB was 60 μM.

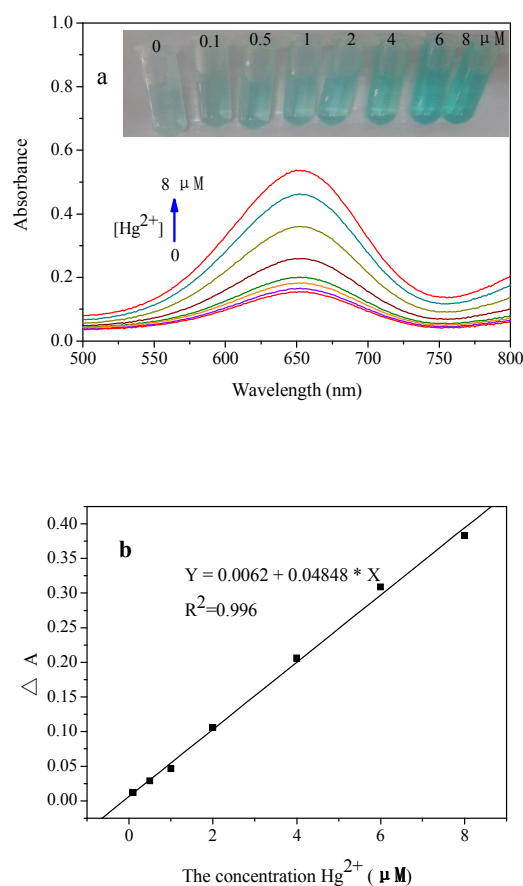


**Fig. 8** The effect of  $\text{Hg}^{2+}$  on the absorption spectra in the TMB/ $\text{MnO}_2$ /GSH system (a), linear calibration plot for  $\text{Hg}^{2+}$  detection, where  $\Delta A = A_{(\text{Hg}^{2+}, 652\text{nm})} - A_{(\text{blank}, 652\text{nm})}$ , (b). Inset: Color changes of TMB/ $\text{MnO}_2$ /GSH system with different concentration of  $\text{Hg}^{2+}$ .

### 3.4. Colorimetric assay for $\text{Hg}^{2+}$ determination

Under the optimum conditions, the changed of the absorbance at 652 nm with different concentration of  $\text{Hg}^{2+}$  were investigated. As it was shown in Fig. 8a, we can observe that the light blue solution become more and more deep and the absorbance values at 652 nm gradually increase with the increasing of  $\text{Hg}^{2+}$  concentration from 0.1  $\mu\text{M}$  to 8.0  $\mu\text{M}$ . Fig. 8b showed that a good linear relationship was obtained between the absorbance and the  $\text{Hg}^{2+}$  concentration in the range from 0.1  $\mu\text{M}$  to 8.0  $\mu\text{M}$  ( $R^2=0.996$ ), and the limit of detection of  $\text{Hg}^{2+}$  was evaluated as 0.08  $\mu\text{M}$ . Compared with other nanomaterial-based colorimetric detection methods for  $\text{Hg}^{2+}$ , the proposed colorimetric method showed a very comparable detection limit (Table 1). In addition, the proposed precise method was calculated by the formula:  $S/N=(\text{average}_{\text{sample}} - \text{average}_{\text{blank}}) / \text{SD}_{\text{blank}}$ . And the sample concentrations consistent with  $3 < S/N < 5$  conditions was defined as limit of detection<sup>36</sup>.

**Table 1** Comparison of different nanoparticle-based colorimetric methods for  $\text{Hg}^{2+}$  detection.

Method	Linear range	Detection limit	References
unmodified silver nanoparticles	10-100 $\mu\text{M}$	2.2 $\mu\text{M}$	30
Bovine serum albumin-Au clusters	10 nM -10 $\mu\text{M}$	3 nM	31
peroxidase-like activity of graphene oxide-gold nanohybrids	0-50 $\mu\text{M}$	300 nM	32
unmodified gold nanoparticle	0.39-8.89 $\mu\text{M}$	200 nM	33
gold nanorods embedded in a functionalized silicate sol-gel matrix	1-7 $\mu\text{M}$	317 nM	34
gold nanoparticles	0.01-5 $\mu\text{M}$	8 nM	35
$\text{MnO}_2$ nanorods	0.1-8.0 $\mu\text{M}$	0.08 $\mu\text{M}$	This work

<sup>a</sup>

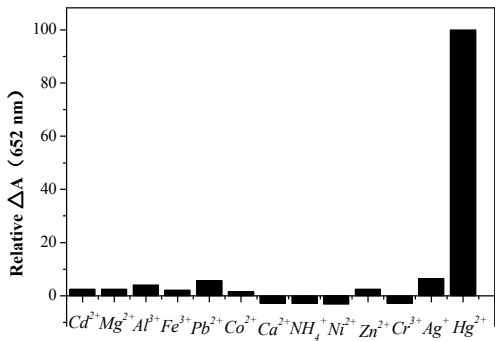


**Fig. 9**  $\Delta A$  response of TMB,  $\text{MnO}_2$  and GSH mixed solution to blank and different common ions in the presence of  $\text{Hg}^{2+}$  (8.0  $\mu\text{M}$ ). The other ions add also 8  $\mu\text{M}$ . Relative  $\Delta A = (\Delta A_{\text{total}} - \Delta A_{\text{Hg}^{2+}}) / \Delta A_{\text{Hg}^{2+}}$

### 3.5. The effects of foreign substances.

To determine the selectivity of the proposed colorimetric method, the effect of coexisting substances on the detection of 8.0  $\mu\text{M}$   $\text{Hg}^{2+}$  was studied under the optimized conditions (GSH, 20  $\mu\text{M}$ ) and mixed ions solution or standard  $\text{Hg}^{2+}$  solution were pre-incubated for 5 min. Then TMB (60  $\mu\text{M}$ ) and  $\text{MnO}_2$  (11.4  $\mu\text{g/mL}$ ) was added in 0.2 M acetate buffer solution (pH 4.5) containing coexisting substances, and the obtained mixed solution was incubated at room temperature for 10 min. The final concentrations of coexisting substances including  $\text{Cd}^{2+}$ ,  $\text{Mg}^{2+}$ ,  $\text{Al}^{3+}$ ,  $\text{Fe}^{3+}$ ,  $\text{Pb}^{2+}$ ,  $\text{Co}^{2+}$ ,  $\text{Ca}^{2+}$ ,  $\text{NH}_4^+$ ,  $\text{Ni}^{2+}$ ,  $\text{Zn}^{2+}$ ,  $\text{Cr}^{3+}$  and  $\text{Ag}^+$  were all 8.0  $\mu\text{M}$ . As shown in Fig. 9, these coexisting substances did not influenced on the determination of  $\text{Hg}^{2+}$  and demonstrated the high selectivity of the TMB/ $\text{MnO}_2$  nanorods/ GSH system for  $\text{Hg}^{2+}$  detection. Therefore, this system would be used to detect  $\text{Hg}^{2+}$  in real samples.

**Table 2** Results for the determination of the mercury ion in two kinds of water samples

Sample	Original amount ( $\mu\text{M}$ )	Added ( $\mu\text{M}$ )	Found ( $\mu\text{M}$ )	Recovery (%)	RSD (%) (n=3)
Pool water	N.D. <sup>a</sup>	0.5	0.41	82	0.44
		2.0	2.02	101	2.5
		4.0	4.28	107	0.67
Li River water	N.D.	0.5	0.455	91	1.4
		2.0	2.16	108	0.49
		4.0	4.56	114	0.57

<sup>a</sup>N.D., not detected

### 3.6. Detection of $\text{Hg}^{2+}$ in real samples.

In order to illustrate the feasibility of the proposed method, it was used to determine  $\text{Hg}^{2+}$  in real samples under the optimal experimental conditions. The results were listed in Table 2. The recovery values of the two samples ranged from 82% to 114%. Hence, this simple and rapid colorimetric method can be considered a useful means for  $\text{Hg}^{2+}$  determination in real samples.

## 4. Conclusion

In summary, a simple, rapid and sensitive colorimetric method was developed for  $\text{Hg}^{2+}$  determination based on “off - on” sensing of colourless TMB molecular recovery to the blue colour TMB cation radicals. In this sensing system  $\text{MnO}_2$  nanorods was prepared and used as oxidase-like mimetic catalytic oxidation of TMB in absence of  $\text{H}_2\text{O}_2$ . The catalytic reaction was fast and the colour change of the reaction system is obviously visible by our naked eyes. The proposed method also has a good linear relationship, the limit of detection and recovery values. Therefore, this novel “off-on” colorimetric method opens up a new possibility for monitoring trace levels of  $\text{Hg}^{2+}$  in water sample.

## Acknowledgement

The financial support from the National Natural Science Foundation of China (21365005) and Guangxi Natural Science Foundation of China (2014GXNSFGA118002) is gratefully acknowledged.

## Notes and references

Key Laboratory for the Chemistry and Molecular Engineering of Medicinal Resources (Ministry of Education of China), College of Chemistry and Pharmaceutical Science of Guangxi Normal University, Guilin 541004, P. R. China.

Corresponding author: Prof. Fanggui Ye

Tel: +86-773-5856104; fax: +86-773-5832294

E-mail address: [fangguiye@163.com](mailto:fangguiye@163.com)

[1] E. M. Nolan and S. J. Lippard, *Chem. Rev.*, 2008, **108**, 3443-3480.

[2] S. Jayabal, R. Sathiyamurthi and R. Ramaraj, *J. Mater. Chem. A*, 2014, **2**, 8918-8925.

[3] J. H. Huang, X. Gao, J. J. Jia, J. K. Kim and Z. Li, *Anal. Chem.*, 2014, **86**, 3209-3215.

[4] M. A. Domínguez, M. Grünhut, M. F. Pistonesi, M. S. Di Nezio, and M. Centurión, *J. Agric. Food Chem.*, 2012, **60**, 4812-4817.

[5] E. Kenduzler, M. Ates, Z. Arslan, M. McHenry and P. B. Tchounwou, *Talanta*, 2012, **93**, 404-410.

[6] S. Cai, K. Lao, C. Lau and J. Lu, *Anal. Chem.*, 2011, **83**, 9702-9708.

[7] F. El Aroui, S. Lahrich, A. Farahi, M. Achak, L. El Gaini, M. Bakasse, A. Bouzidi and M. A. El Mhammedi, *Electroanalysis*, 2014, **26**, 1751-1760.

[8] Q. Zhou, A. Xing and K. Zhao, *J. Chromatogr. A*, 2014, **1360**, 76-81.

[9] D. Wu, X. Huang, X. Deng, K. Wang and Q. Liu, *Anal. Methods*, 2013, **5**, 3023-3027.

[10] D. Sareen, P. Kaur and K. Singh, *Coord. Chem. Rev.*, 2014, **265**, 125-154.

[11] Y. Lin, J. Ren and X. Qu, *Acc. Chem. Res.*, 2014, **47**, 1097-1105.

[12] H. Wei and E. Wang, *Chem. Soc. Rev.*, 2013, **42**, 6060-6093.

[13] Y. J. Long, Y. F. Li, Y. Liu, J. J. Zheng, J. Tang and C. Z. Huang, *Chem. Commun.*, 2011, 47, 11939-11941.

[14] Z. Sun, N. Zhang, Y. Si, S. Li, J. Wen, X. Zhu and H. Wang, *Chem. Commun.*, 2014, **50**, 9196-9199.

[15] Z. Mohammadpour, A. Safavi and M. Shamsipur, *Chem. Eng. J.*, 2014, **255**, 1-7.

[16] W. Lia, B. Chen, H. Zhang, Y. Sun, J. Wang, J. Zhang and Y. Fu, *Biosens. Bioelectron.*, 2015, **66**, 251-258.

[17] J. Liu, X. Hu, S. Hou, T. Wen, W. Liu, X. Zhu and X. Wu, *Chem. Commun.*, 2011, **47**, 10981-10983.

[18] G.-L. Wang, X.-F. Xu, L.-H. Cao, C.-H. He, Z.-J. Li and C. Zhang, *RSC Adv.*, 2014, **4**, 5867-5872.

[19] L. Zhang, J. Lian, L. Wu, Z. Duan, J. Jiang and L. Zhao, *Langmuir*, 2014, **30**, 7006-7013.

[20] R. Chen, J. Yu and W. Xiao, *J. Mater. Chem. A*, 2013, **1**, 11682-11690.

[21] S. Saha and A. Pal, *Sep. Purif. Technol.*, 2014, **134**, 26-36.

[22] Y. Wan, P. Qi, D. Zhang, J. Wu and Y. Wang, *Biosens. Bioelectron.*, 2012, **33**, 69-74.

[23] X. Liu, Q. Wang, H. Zhao, L. Zhang, Y. Su and Y. Lv, *Analyst*, 2012, **137**, 4552-4558.

[24] X. Liu, Q. Wang, Y. Zhang, L. Zhang, Y. Su and Y. Lv, *New J. Chem.*, 2013, **37**, 2174-2178.

[25] Y. Xiong, S. Chen, F. Ye, L. Su, C. Zhang, S. Shen and S. Zhao, *Anal. Methods*, 2015, **7**, 130-1306.

[26] X. Zhang, S. He, Z. Chen and Y. Huang, *J. Agric. Food Chem.*, 2013, **61**, 840-847.

[27] Z. Jiang, Y. Liu, X. Hu and Y. Li, *Anal. Methods*, 2014, **6**, 5647-5651.

[28] M. Ravichandran, *Chemosphere*, 2004, **55**, 319-331.

[29] H.-C. Chang, Y.-F. Chang, N.-C. Fan and J. A. Ho, *ACS Appl. Mater. Interfaces*, 2014, **6**, 18824-18831.

[30] R. Zhu, Y. Zhou, X.-L. Wang, L.-P. Liang, Y.-J. Long, Q.-L. Wang, H.-J. Zhang, X.-X. Huang and H.-Z. Zheng, *Talanta*, 2013, **117**, 127-132.

[31] K. Farhadi, M. Forough, R. Molaeia, S. Hajizadeha and A. Rafipou, *Sens. Actuators, B*, 2012, **161**, 880-885.

[32] X. Chen, N. Zhai, J. H. Snyder, Q. Chen, P. Liu, L. Jin, Q. Zheng, F. Lin, J. Hu and H. Zhou, *Anal. Methods*, 2015, **7**, 1951-1957.

[33] Y. Wang, F. Yang and X. Yang, *Biosens. Bioelectron.*, 2010, **25**, 1994-1998.

[34] S. Jayabal, R. Sathiyamurthi and R. Ramara, *J. Mater. Chem. A*, 2014, **2**, 8918-8925.

[35] Y. Zhou, H. Dong, L. Liu, M. Li, K. Xiao and M. Xu, *Sens. Actuators, B*, 2014, **196**, 106-111.

[36] L. Guo, Y. Xu, A. R. Ferhan, G. Chen and D. Kim, *J. Am. Chem. Soc.*, 2013, **135**, 12338-12345.

Graphical Abstract

